FT-IR study of the interaction of $(\mu\text{-}C_7H_7)FeCo(\mu\text{-}CO)(CO)_4$, $(\eta^4\text{-}C_7H_8)Fe(CO)_3$ and $(\eta^3\text{-}C_7H_7)Co(CO)_3$ with hydroxylated alumina surfaces

Sándor Dobos

Spectroscopic Department, Institute of Isotopes of the Hungarian Academy of Sciences, P.O.B. 77, H-1525 Budapest (Hungary)

and Josef Takats

Department of Chemistry, University of Alberta, Edmonton, Alta., T6G 2G2 (Canada)

Abstract

Surface reactions of $(\mu\text{-}C_7H_7)FeCo(\mu\text{-}CO)(CO)_4$ adsorbed on a hydroxylated alumina surface were followed by FT-IR spectroscopy at room temperature and in the temperature range 303–723 K. At room temperature $(\mu\text{-}C_7H_7)FeCo(\mu\text{-}CO)(CO)_4$ quickly decomposed into physisorbed $(\eta^4\text{-}C_7H_8)Fe(CO)_3$ and surface anchored $[(\eta^5\text{-}C_7H_7)Fe(CO)_2]^+O^-(Al)$; no species with carbonyl groups bonded to Co were detected on the surface. Analogous experiments were performed with $(\eta^4\text{-}C_7H_8)Fe(CO)_3$ and $(\eta^3\text{-}C_7H_7)Co(CO)_3$. The thermal behavior of surface species derived from $(\eta^4\text{-}C_7H_8)Fe(CO)_3$ was practically identical with that of the species obtained from $(\mu\text{-}C_7H_7)FeCo(\mu\text{-}CO)(CO)_4$. However, $(\eta^3\text{-}C_7H_7)Co(CO)_3$ decomposed readily on the surface already at room temperature and yielded oxidized, surface cobalt species with no carbon monoxide.

Introduction

Recently one of us reported FT-IR studies on the interaction of the $[(\eta\text{-}C_5H_5)M(CO)_2]_2$ (M = Fe, Ru) and $(\eta\text{-}C_5H_5)Fe(CO)_2I$ molecules with hydroxylated alumina and silica surfaces [1–3]. Several surface anchored $CpM(CO)_x$ (x = 2, 1) complexes of differing stability were identified. In the case of $[(\eta\text{-}C_5H_5)Fe(CO)_2]_2$ the large number and considerable stability of the surface species were in contrast to the surface behavior of pure iron carbonyl clusters which very quickly lost all carbonyl ligands while the iron atoms became oxidized, due to the rather reactive nature of the hydroxylated oxide surfaces and also because during sample preparation short contacts with atmospheric oxygen were unavoidable [4, 5]. The stabilizing effect of the cyclopentadienyl ligands was quite dramatic. Some of the surface iron species were stable even when kept in air for weeks.

The stabilizing role of the cyclopentadienyl ring is most probably the result of steric protection, but electronic factors, like the strong bonding of the ligand may also be involved. In either case, the natural extension to investigate this interesting phenomenon is to perform experiments with iron carbonyl compounds that contain unsaturated, cyclic organic ligands of different sizes and of different bonding capabilities.

The subject of the present report is an analogous study of the surface reactions of $(\mu\text{-}C_7H_7)FeCo(\mu\text{-}CO)(CO)_4$, where Fe (and Co) is bonded to a ligand that is larger in size and is bonded differently from the cyclopentadienyl moiety and occupies a special bridging position between Fe and a second metal, Co. Complementary experiments with $(\eta^4\text{-}C_7H_8)Fe(CO)_3$ and $(\eta^3\text{-}C_7H_7)Co(CO)_3$ were undertaken to serve as references in the assignment of the surface species derived from the bimetallic $(\mu\text{-}C_7H_7)FeCo(\mu\text{-}CO)(CO)_4$ complex and for comparison of the stability of the mono- and heterobinuclear Fe and Co cycloheptatrienyl compounds toward the hydroxylated alumina surfaces. In the study of pure cobalt carbonyl clusters (mainly $Co_2(CO)_8$ and $Co_4(CO)_{12}$), *in situ* impregnation is generally used [6–11] in order to avoid contact with oxygen, which quickly oxidizes the Co center and results in the loss of all carbonyl ligands in a manner analogous to binary iron carbonyls. Therefore the present study is also useful for testing the influence of cyclic organic ligands on the nature and stability of surface cobalt species.

Experimental

$(\eta^4\text{-}C_7H_8)Fe(CO)_3$, $(\eta^3\text{-}C_7H_7)Co(CO)_3$ and $(\mu\text{-}C_7H_7)FeCo(\mu\text{-}CO)(CO)_4$ were prepared according to

the procedures given in refs. 12–14. The compounds were deposited on alumina (Degussa, Alon C) from pentane solution to an extent of c. 0.05 and/or c. 0.5 wt.%. Prior to impregnation the support was heated in vacuum at 433 K for 12 h. This pretreatment eliminates the adsorbed water. However, the surface remains almost completely hydroxylated.

Three types of experiments were performed.

(i) After impregnation, the supported complex was dried in vacuum for 5 min, and wetted with paraffin oil (Nujol mull). Air exposure of the compound was about 10 s in this case. The IR spectrum of the suspension was then recorded between two KBr windows. As described elsewhere [4, 5] the presence of paraffin oil slows down the surface reactions and, therefore, information can be obtained about the very first steps of complex–support interaction. IR spectra were recorded at room temperature.

(ii) In the second method, the supported complexes were dried under vacuum for 12 h and then pressed into wafers (10 mg/cm^2) which were placed into a heatable vacuum IR cell. IR spectra, under vacuum and in a dihydrogen atmosphere, were recorded at temperatures ranging from 303 to 723 K. It is important to note that the sample was exposed to air for a certain period of time when the wafers were pressed. The wafer for the experiment under vacuum was prepared first and this time the sample was exposed to air for about 15–20 min. After having finished this experiment another wafer was prepared for the experiment under dihydrogen atmosphere and the supported complex was exposed to air for a further 15–20 min. Thus the sample used in the H$_2$ experiment was in contact with air twice as long as the one used in the experiment under vacuum.

(iii) In this method we combined the procedures of (i) and (ii). Part of the sample, prepared as described in method (ii), was also measured in Nujol mull immediately after the 12 h drying period. In this experiment the contact with air was only about 10 s.

The IR measurements were performed using Bomem MB-102 and Nicolet MX-1 FTIR spectrometers. Spectra of similarly pretreated alumina in Nujol mull or spectra of wafers of the pure oxide recorded at different temperatures were used as references.

Results

In Fig. 1, the spectra of the $(\mu$-C$_7$H$_7)$FeCo$(\mu$-CO)(CO)$_4$, $(\eta^4$-C$_7$H$_8)$Fe(CO)$_3$ and $(\eta^3$-C$_7$H$_7)$Co(CO)$_3$ in pentane solutions are shown.
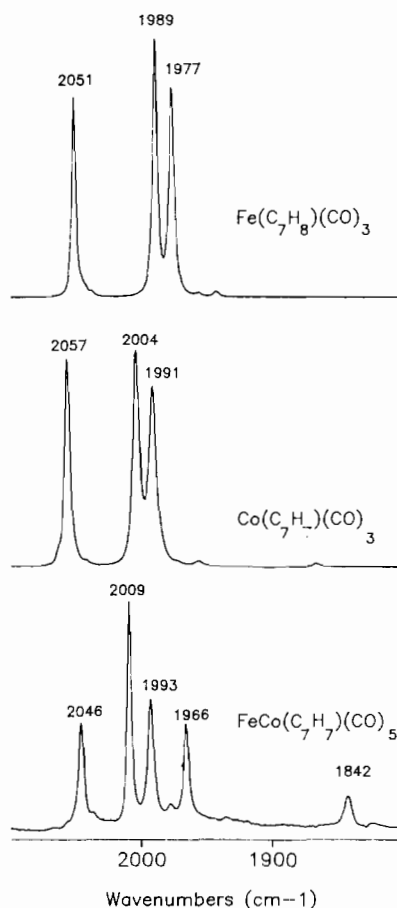
Fig. 1. FT-IR spectra of $(\mu$-C$_7$H$_7)$FeCo$(\mu$-CO)(CO)$_4$, $(\eta^4$-C$_7$H$_8)$Fe(CO)$_3$ and $(\eta^3$-C$_7$H$_7)$Co(CO)$_3$ in pentane solutions.

Experiments with Al$_2$O$_3$ wafers under vacuum and in H$_2$ atmosphere

$(\mu$-C$_7$H$_7)$FeCo$(\mu$-CO)(CO)$_4$

In Fig. 2(a) the spectra recorded at different temperatures in vacuum are seen, while Fig. 3(a) shows those recorded under H$_2$ atmosphere. The metal loading is c. 0.5% which corresponds to about one (1) monolayer of coverage. The room temperature spectrum represents the surface species which developed during a 12 h drying period plus brief contact with air during the pressing of the wafer. Both series of spectra are similar, the thermal behaviors are alike in vacuum and under H$_2$ atmosphere. The main feature of the spectra is a triad consisting of a strong band at about 2050–52, a very strong broad band at 1988 and a hardly discernable shoulder around 1960 cm^{-1}. Another characteristic feature is the weaker doublet with bands at c. 2070 and 2010 cm^{-1}. The surface species producing the doublet is less stable (see also the difference spectra in Figs. 2(b) and 3(b)) and it disappears above 373 K, while the main triad is present up to 433 K. The difference spectra show negative peaks only. The fact
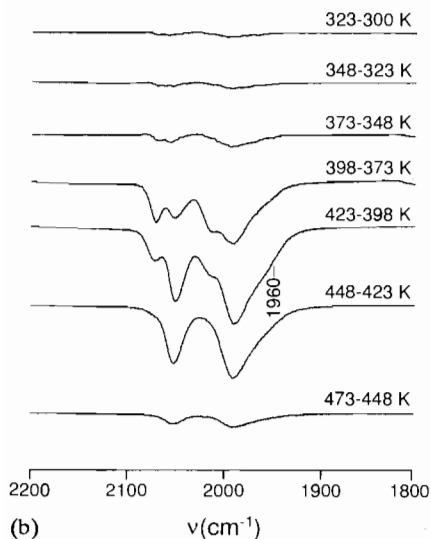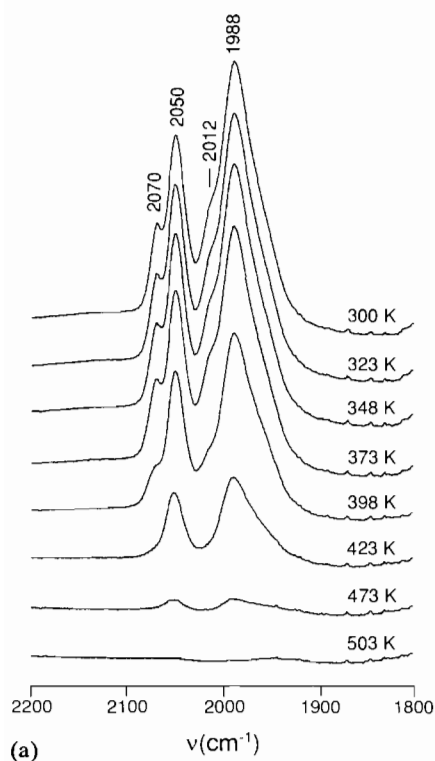
Fig. 2. FT-IR spectra (a) and difference spectra (b) of the $(\mu\text{-}C_7H_7)FeCo(\mu\text{-}CO)(CO)_4/Al_2O_3$ system during thermal treatment under vacuum, 0.5% metal loading.

Fig. 3. FT-IR spectra (a) and difference spectra (b) of the $(\mu\text{-}C_7H_7)FeCo(\mu\text{-}CO)(CO)_4/Al_2O_3$ system during thermal treatment in H_2 atmosphere, 0.5% metal loading.

that no positive peaks are seen indicates that there is no interconversion between the different species on the surface during the thermal treatment.

The spectra in Figs. 4(a) (vacuum) and 5(a) (H_2 atmosphere) were recorded on analogous samples, however, with 0.05% metal loading. At such a low metal loading the surface coverage is presumed to be a small fraction of a monolayer (c. 0.1), making it possible for all the adsorbed molecules to have much easier access
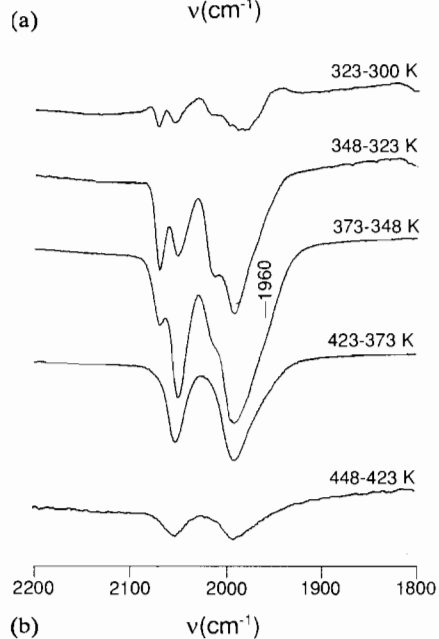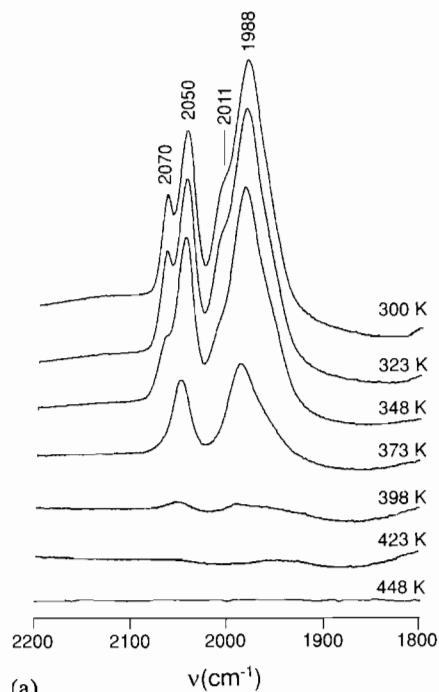
to surface active sites. Under this condition the patterns of the spectra are somewhat different, indicating different or differently bonded surface species. Two pairs of bands are distinguishable: the first doublet at 2066 and 1996 cm^{-1}, the second at 2044 and 1966 cm^{-1}. The surface species belonging to the higher frequency pair is more stable under vacuum, while the species belonging to the lower frequency bands is more stable under hydrogen atmosphere. In general, the stability range of both species is considerably higher (about

10
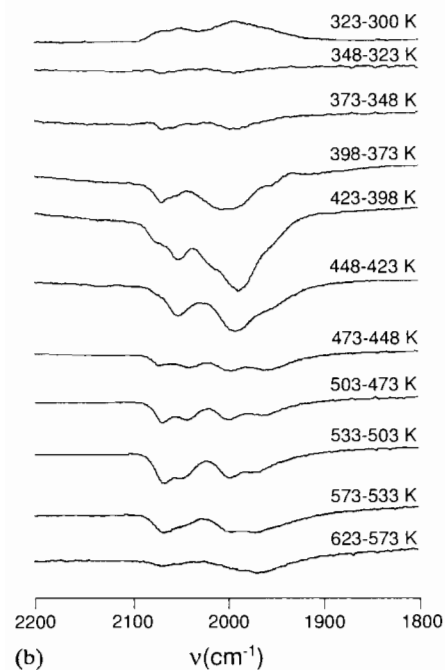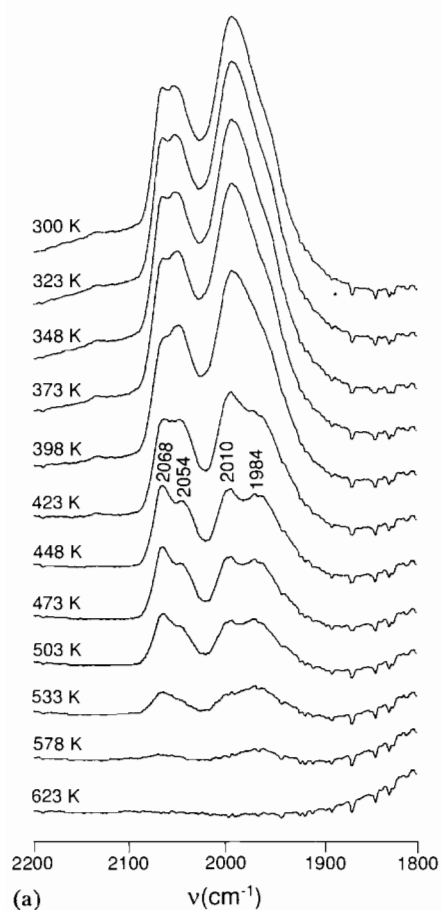
Fig. 4. FT-IR spectra (a) and difference spectra (b) of the $(\mu\text{-}C_7H_7)FeCo(\mu\text{-}CO)(CO)_4/Al_2O_3$ system during thermal treatment under vacuum, 0.05% metal loading.

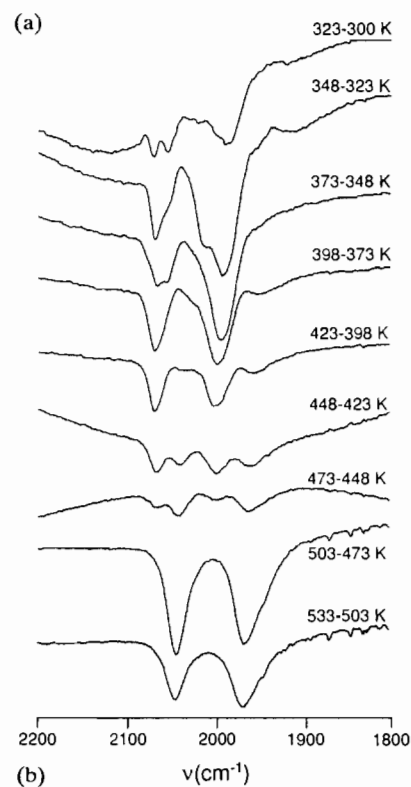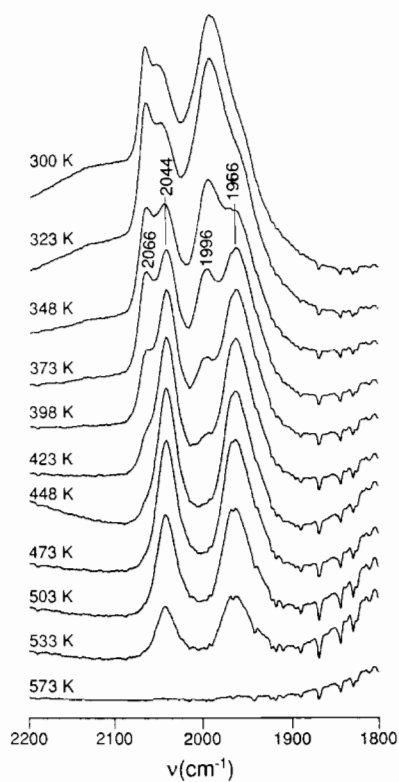Fig. 5. FT-IR spectra (a) and difference spectra (b) of the $(\mu\text{-}C_7H_7)FeCo(\mu\text{-}CO)(CO)_4/Al_2O_3$ system during thermal treatment in H_2 atmosphere, 0.05% metal loading.

100–150 K) than that of the species developed from samples with high metal loading. Surface carbonyl species are detected in both cases up to 533–573 K. The higher stability of the latter species suggests that, although there is a similarity in the band frequencies, they must be different from those found in the case of high metal loading. The different thermal behaviors of these species under vacuum and in H_2 atmosphere suggest the possible coexistence of carbonyl ligands bonded to metals in different oxidation states, as observed previously in the case of ruthenium dicarbonyls [4, 5]. However, if this is the case the interconversion between the forms is not as obvious as with the $Ru^{0-I}(CO)_2$ fragment. There are no positive peaks in the difference spectra (Figs. 4(b) and 5(b)) which would indicate the formation of one or both carbonyls during the heating process. Instead, both species decrease on heating.
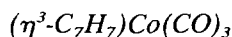
$(\eta^4\text{-}C_7H_8)Fe(CO)_3$
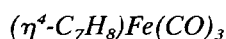
Figures 6(a) and 7(a) show the spectra recorded at different temperatures under vacuum and in H_2 atmosphere, respectively. The metal loading was c. 0.5%. Just as in the above cases, the room temperature spectrum represents the surface species which developed during the 12 h drying, plus the contact period with air during the pressing of the wafer.

It is evident that the spectra of supported (η^4-$C_7H_8)Fe(CO)_3/Al_2O_3$ samples are in general similar to those of (μ-$C_7H_7)FeCo(\mu$-$CO)(CO)_4/Al_2O_3$ with high metal loading (Figs. 2(a) and 3(a)). The main feature is again a strong band at 2052–54 cm^{-1} and a very strong band at 1982–84 cm^{-1}, however the expected shoulder at around 1960 cm^{-1} is no longer visible. The other characteristic feature is the weaker doublet with bands at 2066–68 and 2008–10 cm^{-1}. The thermal behaviour and stability ranges of the species belonging to the above band systems, in general, are also similar.

Besides the general similarities, there are some small differences between the spectra of supported (η^4-$C_7H_8)Fe(CO)_3/Al_2O_3$ and (μ-$C_7H_7)FeCo(\mu$-$CO)(CO)_4/Al_2O_3$ systems. At lower temperatures supported (η^4-$C_7H_8)Fe(CO)_3/Al_2O_3$ shows some spectral features which are not present in the spectra of the supported (μ-$C_7H_7)FeCo(\mu$-$CO)(CO)_4/Al_2O_3$ (compare difference spectra in Figs. 2(b), 3(b) and 6(b), 7(b)).

Nevertheless, the similarities are dominant and suggest that the main surface carbonyl species obtained from (μ-$C_7H_7)FeCo(\mu$-$CO)(CO)_4/Al_2O_3$ might contain carbonyl ligands bonded to Fe only.

$(\eta^3\text{-}C_7H_7)Co(CO)_3$

We found that the spectra of supported (η^3-$C_7H_7)Co(CO)_3/Al_2O_3$ samples (metal loading of c. 0.5%) contained no bands in the spectral region of 2200–1700

Fig. 6. FT-IR spectra (a) and difference spectra (b) of the $(\eta^4\text{-}C_7H_8)Fe(CO)_3/Al_2O_3$ system during thermal treatment under vacuum, 0.5% metal loading.

cm^{-1}. Thus the samples contained no detectable carbonyls, which means that $(\eta^3\text{-}C_7H_7)Co(CO)_3$ is not stable under the conditions used to prepare the wafers, 12 h drying and contact period with air while pressing the wafer. This result seems to support the conclusions reached above on the basis of the spectra in Figs. 6 and 7, that only iron containing carbonyls exist on the surface of supported (μ-$C_7H_7)FeCo(\mu$-$CO)(CO)_4/Al_2O_3$ systems. As we will see later, the absence of
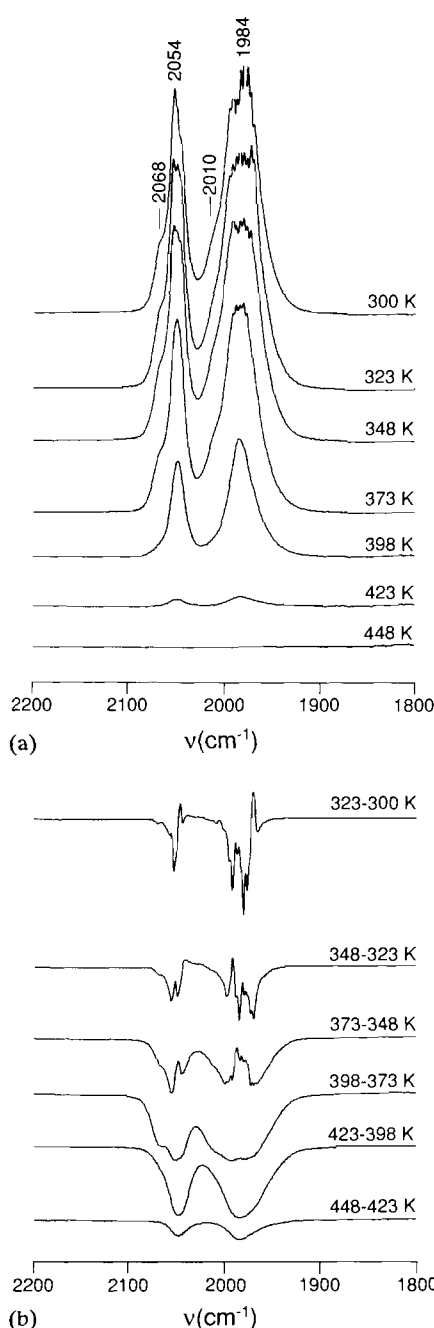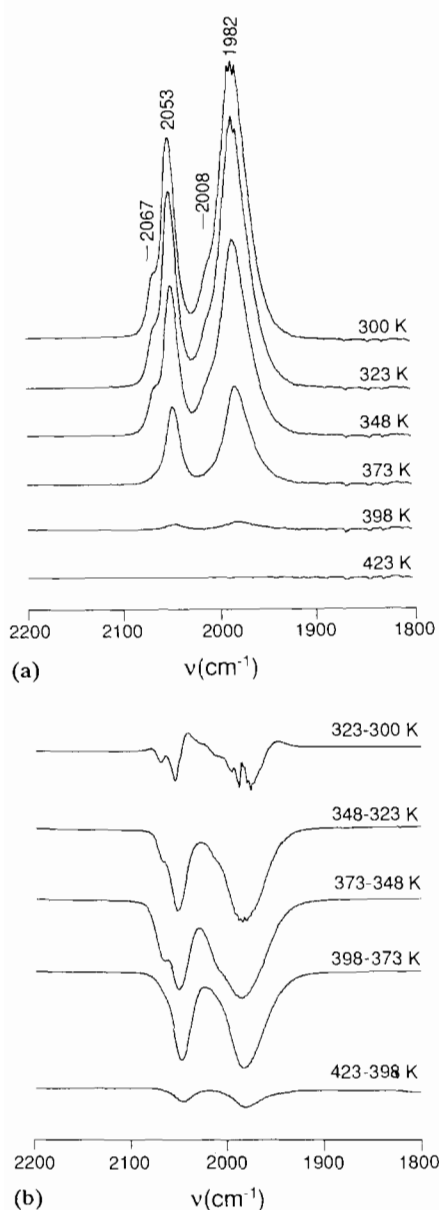
(a)

ν(cm⁻¹)

(b)

ν(cm⁻¹)

Fig. 7. FT-IR spectra (a) and difference spectra (b) of the $(\eta^4\text{-}C_7H_8)Fe(CO)_3/Al_2O_3$ system during thermal treatment in H_2 atmosphere, 0.5% metal loading.

any Co subcarbonyls is not due to the rather long contact time with air, the decomposition of $(\eta^3\text{-}C_7H_7)Co(CO)_3$ is already complete during the 12 h drying period under vacuum.

Experiments with the complexes adsorbed on Al_2O_3/Nujol systems

  Immediately after impregnation

  The spectrum of the $(\mu\text{-}C_7H_7)FeCo(\mu\text{-}CO)(CO)_4$/$Al_2O_3$/Nujol system with a metal loading of *c*. 0.5%, recorded at room temperature using a sample that was wetted with paraffin oil (Nujol mull) is shown in Fig. 8(a), and it represents, as already mentioned, the result

(a)

(b)

(c)

(d)

ν(cm⁻¹)
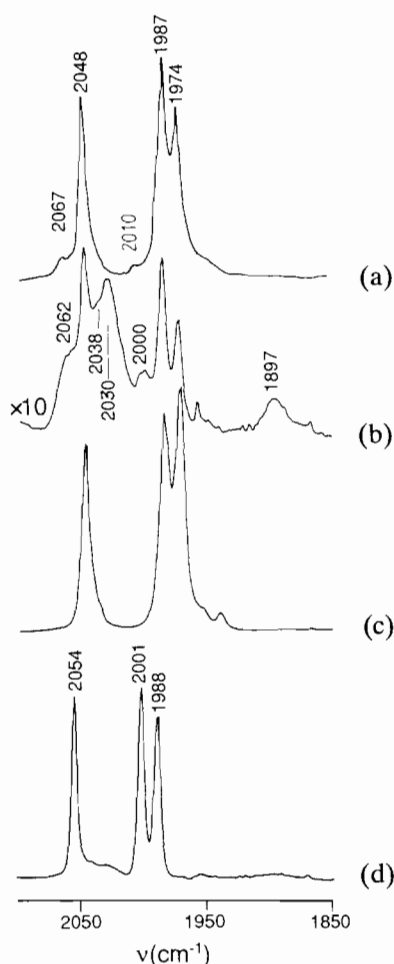
Fig. 8. FT-IR spectra recorded in Nujol mull immediately after impregnation: (a) $(\mu\text{-}C_7H_7)FeCo(\mu\text{-}CO)(CO)_4/Al_2O_3$/Nujol system, 0.5% metal loading; (b) $(\mu\text{-}C_7H_7)FeCo(\mu\text{-}CO)(CO)_4/Al_2O_3$/Nujol system, 0.05% metal loading; (c) $(\eta^4\text{-}C_7H_8)Fe(CO)_3/Al_2O_3$/Nujol system; (d) $(\eta^3\text{-}(C_7H_7)Co(CO)_3/Al_2O_3$/Nujol system.

of the first steps of surface–complex interaction. First, it should be mentioned that in Nujol mull there is no change in the appearance of the spectrum during the first two hours. In the Figure only the spectrum recorded at time zero is shown. Taking into account that in this type of experiment the supported system was exposed to air for only a very short period of time (*c*. 10 s) before being wetted and, in this way, was also protected from air by the paraffin oil, we expected that unreacted, only physisorbed $(\mu\text{-}C_7H_7)FeCo(\mu\text{-}CO)(CO)_4$ molecules on Al_2O_3 or at least species with carbonyls bonded to Co would also be detected. This was not the case. No unchanged, physisorbed $(\mu\text{-}C_7H_7)FeCo(\mu\text{-}CO)(CO)_4$ could be seen, i.e. there was no evidence of any bridging CO group in the 1850–1820 cm⁻¹ range. Further, there was no band in the 2010–2000 cm⁻¹ range either, where the strongest band of the unperturbed $(\mu\text{-}C_7H_7)FeCo(\mu\text{-}CO)(CO)_4$ is expected. The very strong, sharp bands at 2049, 1987 and 1975 cm⁻¹ can be assigned to adsorbed

---

$(\eta^4\text{-}C_7H_8)Fe(CO)_3$, and indeed these frequencies compare favorably with those obtained from the $(\eta^4\text{-}C_7H_8)Fe(CO)_3/Al_2O_3/Nujol$ system (Fig. 8(c)). Furthermore, no bands due to $(\eta^3\text{-}C_7H_7)Co(CO)_3$ were detected either, as is evident from comparison of Figs. 8(a) and 8(d); $(\mu\text{-}C_7H_7)FeCo(\mu\text{-}CO)(CO)_4/Al_2O_3/Nujol$ and $(\eta^3\text{-}C_7H_7)Co(CO)_3/Al_2O_3/Nujol$ systems, respectively. Figure 8(d) provides evidence that $(\eta^3\text{-}C_7H_7)Co(CO)_3$ is not immediately decomposed after impregnation. Consequently, if it is formed from $(\mu\text{-}C_7H_7)FeCo(\mu\text{-}CO)(CO)_4$ during impregnation it shouldn't immediately decompose and so its frequencies (which are about 6–16 cm^{-1} higher than those of $(\eta^4\text{-}C_7H_8)Fe(CO)_3$) should also be observed in Fig. 8(a). As stated above, this is not the case. However, as can be seen in Fig. 8(b), at very low concentration (metal loading c. 0.05%), besides $(\eta^4\text{-}C_7H_8)Fe(CO)_3$, some other intermediates can also be traced to the reaction of $(\mu\text{-}C_7H_7)FeCo(\mu\text{-}CO)(CO)_4$ with the surfaces. The presence of a band at 1897 cm^{-1} in Fig. 8(b) is very informative as to the plausible nature of this species. This band can be assigned, with reasonable certainty, to a CO group in bridging position. However, its rather high frequency mitigates against the presence of a symmetrical bridging unit and we favor a rather asymmetric, 'incipient' bridging carbonyl moiety [5], where the CO group is shifted towards the Fe atom. This bridging CO band together with the remaining bands (2062w, 2038vw, 2030s and 2000m cm^{-1}) indicate the very likely presence of the $(\mu\text{-}C_7H_7)FeCo(\mu\text{-}CO)(CO)_4$ molecule, however in a highly distorted fashion. The next step in the surface reaction must be the splitting of the metal–metal bond and the formation of $(\eta^4\text{-}C_7H_8)Fe(CO)_3$ (confirmed by the IR bands at 2048, 1987 and 1974 cm^{-1}) and some cobalt subcarbonyl(s) which, however, are unstable and quickly decompose. As discussed above, the splitting of the metal–metal bond does not produce $(\eta^3\text{-}C_7H_7)Co(CO)_3$.

After 12 h drying period under vacuum

The spectra discussed above reflect the stages of the surface reactions immediately after impregnation. Contact with air in these experiments occurred only briefly (10 s). On the other hand, in the experiments performed in the heatable cell using self-supporting wafers, there is a 12 h drying period, and there is also a considerably longer (15–20 min) contact with air. It may happen that this contact with air is long enough to induce some significant reactions in addition to those occurring during the long 12 h drying process. In order to ascertain whether this was the case or not, a part of the sample was measured immediately after the 12 h drying in Nujol mull. In this case the contact time with air was very short, c. 10 s. The spectra for the $(\mu\text{-}C_7H_7)FeCo(\mu\text{-}CO)(CO)_4$ (0.5% metal loading), $(\eta^4\text{-}C_7H_8)Fe(CO)_3$ and
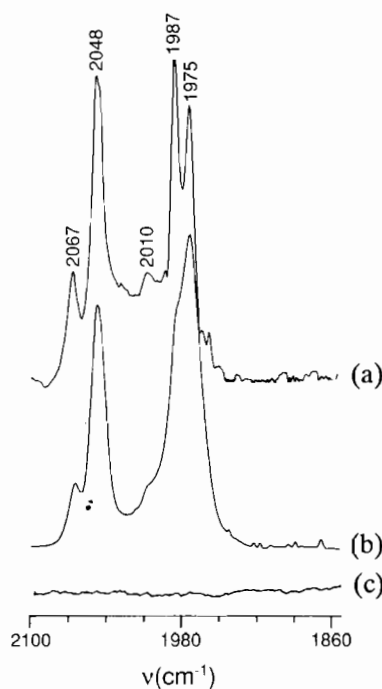
Fig. 9. FT-IR spectra recorded in Nujol mull on samples which were dried after impregnation for 12 h: (a) $(\mu\text{-}C_7H_7)FeCo(\mu\text{-}CO)(CO)_4/Al_2O_3/Nujol$ system, 0.5% metal loading; (b) $(\eta^4\text{-}C_7H_8)Fe(CO)_3/Al_2O_3/Nujol$ system; (c) $(\eta_3\text{-}C_7H_7)Co(CO)_3/Al_2O_3/Nujol$ system.

$(\eta^3\text{-}C_7H_8)Co(CO)_3$ are shown in Fig. 9. In the case of $(\eta^3\text{-}C_7H_7)Co(CO)_3$ no carbonyl bands (Fig. 9(c)) were found, which means that the compound totally decomposed during the 12 h drying period under vacuum. The main feature of the spectra of the Fe–Co and Fe compounds is the triad of bands at 2048, 1987 and 1975 cm^{-1}, indicating that the main surface species immediately after the 12 h vacuum drying process is the same $(\eta^4\text{-}C_7H_8)Fe(CO)_3$. The frequencies of $(\eta^4\text{-}C_7H_8)Fe(CO)_3$ observed here, and in the other type of experiments (see Figs. 2–8), are very close to or even identical with the frequencies of $(\eta^4\text{-}C_7H_8)Fe(CO)_3$ in solution (Fig. 1). The shapes and relative intensities of the bands, however, are sometimes different in the different experiments or at different stages of an experiment.

Finally, it should be noted that there is another pair of bands observed in the cases of $(\mu\text{-}C_7H_7)FeCo(\mu\text{-}CO)(CO)_4$ and $(\eta^4\text{-}C_7H_8)Fe(CO)_3$, at 2067 and 2010 cm^{-1}. A similar pair of bands has also been detected in the thermal treatment experiments, but at somewhat higher frequencies.

Discussion and conclusions

The spectral data and plausible assignments are collected in Table 1.

TABLE 1. Spectral data of surface species derived from $(\mu\text{-}C_7H_7)FeCo(\mu\text{-}CO)(CO)_4$, $(\eta^4\text{-}C_7H_8)Fe(CO)_3$ and $(\eta^3\text{-}C_7H_7)Co(CO)_3$, and those of some reference complexes

Structure	Frequencies	Conditions	Remarks
$(\mu\text{-}C_7H_7)FeCo(\mu\text{-}CO)(CO)_4$	2046 2009 1993 1966 1842	in pentane	highly distorted
$(\eta^4\text{-}C_7H_8)Fe(CO)_3$	2051 1989 1976	in hexane	
$(\eta^3\text{-}C_7H_7)Co(CO)_3$	2057 2004 1992	in hexane	
$(\mu\text{-}C_7H_7)FeCo(\mu\text{-}CO)(CO)_4$ (chemisorbed)	2062 2038 2030 2000 1897	$(\mu\text{-}C_7H_7)FeCo(\mu\text{-}CO)(CO)_4/Al_2O_3/Nujol$	
$(\eta^4\text{-}C_7H_8)Fe(CO)_3$ (physisorbed)	2049 1987 1975	$(\eta^4\text{-}C_7H_8)Fe(CO)_3/Al_2O_3/Nujol$	
	2048 1987 1974	$(\mu\text{-}C_7H_7)FeCo(\mu\text{-}CO)(CO)_4/Al_2O_3/Nujol$	high metal load
	2048 1987 1974	$(\mu\text{-}C_7H_7)FeCo(\mu\text{-}CO)(CO)_4/Al_2O_3/Nujol$	low metal load
	2048 1987 1975	$(\mu\text{-}C_7H_7)FeCo(\mu\text{-}CO)(CO)_4/Al_2O_3/12$ h drying in vac./Nujol	high metal load
	2050 1988 (1960)	$(\mu\text{-}C_7H_7)FeCo(\mu\text{-}CO)(CO)_4/Al_2O_3$ vac., T	high metal load
	2051 1988 (1960)	$(\mu\text{-}C_7H_7)FeCo(\mu\text{-}CO)(CO)_4/Al_2O_3$ H_2, T	high metal load
	2047 1972[a]	$(\mu\text{-}C_7H_7)FeCo(\mu\text{-}CO)(CO)_4/Al_2O_3$ vac., T	low metal load
	2044 1966[a]	$(\mu\text{-}C_7H_7)FeCo(\mu\text{-}CO)(CO)_4/Al_2O_3$ H_2, T	low metal load
	2054 1984	$(\eta^4\text{-}C_7H_8)Fe(CO)_3/Al_2O_3$ vac., T	
	2053 1982	$(\eta^4\text{-}C_7H_8)Fe(CO)_3/Al_2O_3$ H_2, T	
$[(\eta^5\text{-}C_7H_{7/9})Fe(CO)_2]^+O^-(Al)$ (surface bonded)	not observed	$(\eta^4\text{-}C_7H_8)Fe(CO)_3/Al_2O_3/Nujol$	
	2067 2010	$(\mu\text{-}C_7H_7)FeCo(\mu\text{-}CO)(CO)_4/Al_2O_3/Nujol$	high metal load
	not observed	$(\mu\text{-}C_7H_7)FeCo(\mu\text{-}CO)(CO)_4/Al_2O_3/Nujol$	low metal load
	2067 2010	$(\mu\text{-}C_7H_7)FeCo(\mu\text{-}CO)(CO)_4/Al_2O_3/Nujol$	high metal load
	2067 2010	$(\eta^4\text{-}C_7H_8)Fe(CO)_3/Al_2O_3/12$ h drying in vac./Nujol	
	2069 2012	$(\mu\text{-}C_7H_7)FeCo(\mu\text{-}CO)(CO)_4/Al_2O_3$ vac., T	high metal load
	2070 2011	$(\mu\text{-}C_7H_7)FeCo(\mu\text{-}CO)(CO)_4/Al_2O_3$ H_2, T	high metal load
	2066 1995[b]	$(\mu\text{-}C_7H_7)FeCo(\mu\text{-}CO)(CO)_4/Al_2O_3$ vac., T	low metal load
	2066 1996[b]	$(\mu\text{-}C_7H_7)FeCo(\mu\text{-}CO)(CO)_4/Al_2O_3$ H_2, T	low metal load
	2068 2010	$(\eta^4\text{-}C_7H_8)Fe(CO)_3/Al_2O_3$ vac., T	
	2067 2008	$(\eta^4\text{-}C_7H_8)Fe(CO)_3/Al_2O_3$ H_2, T	
$[(\eta\text{-}C_5H_5)Fe(CO)_2]^+O^-(Al)$	2062 2015	$[(\eta\text{-}C_5H_5)Fe(CO)_2]_2/Al_2O_3$ V, T	
$(\eta^3\text{-}C_7H_7)Co(CO)_3$ (physisorbed)	2054 2001 1988	$(\eta^3\text{-}C_7H_7)Co(CO)_3/Al_2O_3/Nujol$	ref. 1

[a]Frequencies at 448 K; see also the text. [b]Frequencies at 373 K; see also the text.

Main surface species: physisorbed $(\eta^4\text{-}C_7H_8)Fe(CO)_3$

It is clear that the interaction of both (μ-$C_7H_7)FeCo(\mu\text{-}CO)(CO)_4$ and $(\eta^4\text{-}C_7H_8)Fe(CO)_3$ with hydroxylated alumina surfaces results in the formation of $(\eta^4\text{-}C_7H_8)Fe(CO)_3$ as the main surface species. The differences in the shapes of the three characteristic bands of $(\eta^4\text{-}C_7H_8)Fe(CO)_3$ in the different systems may be explained by assuming the presence of molecules with slightly different geometries.
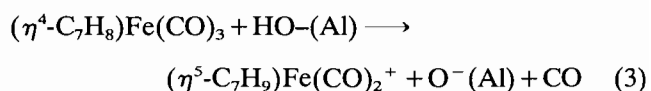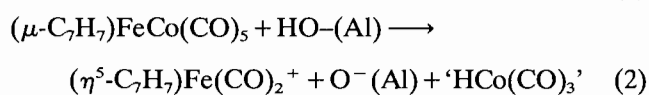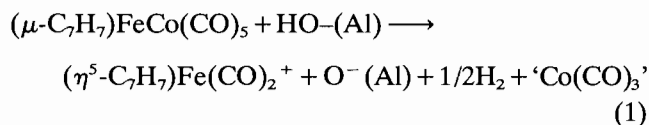
In non-polar solvent, the isolated $(\eta^4\text{-}C_7H_8)Fe(CO)_3$ molecule has a sharp band at 2051 and a well separated doublet at 1989 and 1976 cm^{-1}, which under local C_s symmetry for the $Fe(CO)_3$ group correspond to the a' and a' + a'' symmetry vibrations, respectively. If, under the influence of the molecular environment, the three carbonyls become nearly equivalent, that is the local symmetry approaches C_{3v}, then the doublet becomes less well resolved and at the C_{3v} limit it collapses to a broad band (the degenerate e mode). Thus it is possible to follow changes in the local symmetry of the $Fe(CO)_3$ moiety in the IR spectra. For instance, during the thermal treatment experiments of (μ-C_7H_7)-$FeCo(CO)_5$ and $(\eta^4\text{-}C_7H_8)Fe(CO)_3$ pressed into self-supporting wafer (Figs. 2–3), the doublet is practically not resolved, possibly implying a change in local symmetry. However, the analogous spectra in Nujol mulls show a well resolved doublet. In our experience this type of phenomenon occurs when the surface species in only weakly physisorbed. In the presence of a large amount of paraffin oil, the environment of the molecules mainly consists of apolar paraffin molecules and the perturbation effect of the polar surface is screened, the physisorbed molecules being in a solution-like state. In a wafer, due to the polar environment, the molecules are always more perturbed. Consequently, the bands are broader and the local symmetry may also change, in our case from C_s to close to C_{3v} causing the collapse of the a' and a'' components into the degenerate e band. Therefore, using the Nujol technique, spectral features of physisorbed molecules may be enhanced. Surface anchored species are not as sensitive as physisorbed molecules [5]. For instance, the shape of the pair of bands around 2070 and 2010 cm^{-1} does not show a change, suggesting that it belongs to a surface anchored species.

The fact that the changes in the frequencies of $(\eta^4\text{-}C_7H_8)Fe(CO)_3$ on the alumina surface are very small (2–3 cm^{-1}) suggest that the molecule is bonded to the surface by very weak physisorption, only.

The thermal stability range of physisorbed $(\eta^4\text{-}C_7H_8)Fe(CO)_3$ is 448 K in vacuum and 423 K in a hydrogen atmosphere.

Surface bonded cycloheptatrienyl iron carbonyl fragments

Irrespective of the precursor used, (μ-C_7H_7)-$FeCo(CO)_5$ or $(\eta^4\text{-}C_7H_8)Fe(CO)_3$, the IR spectra exhibit two other bands close to those of surface adsorbed $(\eta^4\text{-}C_7H_8)Fe(CO)_3$, at c. 2070 and 2010 cm^{-1}, respectively. The intensities of these bands range from medium in the Fe–Co experiments with high metal loading (Figs. 2 and 3), to weak in the experiments with $(\eta^4$-$C_7H_8)Fe(CO)_3$ (Figs. 6 and 7). Since pure iron carbonyls are known not to be stable on alumina surfaces, these bands must be assigned to some cycloheptatrienyl iron carbonyl fragments and the higher frequencies suggest that the iron center is oxidized. The angle between the CO groups, calculated from the relative intensities of the bands, is about 90° if an $Fe(CO)_2$ model fragment is assumed, while an $Fe(CO)_3$ fragment gives the less realistic value of 75°. We suggest that this pair of bands is due to surface anchored $(\eta^5\text{-}C_7H_{7/9})Fe(CO)_2{}^+$ type molecules [15, 16], which could arise either via oxidation of the iron center by surface OH groups (eqn. (1)) or via protonation induced heterolytic cleavage of the Fe–Co bond (eqn. (2)). Protonation of the neutral $(\eta^4$-$C_7H_8)Fe(CO)_3$ will also result in a cationic cycloheptadienyl complex (eqn. (3)), a behaviour well documented in solution [16]. As reported elsewhere [2], analogous surface species with a cyclopentadienyl ligand [$(\eta^5$-$C_5H_5)Fe(CO)_2$-O-] have been postulated on an

$$(\mu\text{-}C_7H_7)FeCo(CO)_5 + HO\text{--}(Al) \longrightarrow$$

$$(\eta^5\text{-}C_7H_7)Fe(CO)_2{}^+ + O^-(Al) + 1/2H_2 + \text{`}Co(CO)_3\text{'} \tag{1}$$

$$(\mu\text{-}C_7H_7)FeCo(CO)_5 + HO\text{--}(Al) \longrightarrow$$

$$(\eta^5\text{-}C_7H_7)Fe(CO)_2{}^+ + O^-(Al) + \text{`}HCo(CO)_3\text{'} \tag{2}$$

$$(\eta^4\text{-}C_7H_8)Fe(CO)_3 + HO\text{--}(Al) \longrightarrow$$

$$(\eta^5\text{-}C_7H_9)Fe(CO)_2{}^+ + O^-(Al) + CO \tag{3}$$

alumina support and exhibit frequencies very similar (2062 and 2015 cm^{-1}) to those observed here. The analogies extend to the thermal stabilities of both type of surface species as well, 398 K for the $C_7H_{7/9}$ (see Figs. 2 and 6) and 393 K for the cyclopentadienyl bonded compounds. Under a hydrogen atmosphere the cationic species disappear at a somewhat lower temperature, c. 373 K (see Figs. 3 and 7).

Traces of surface bonded $(\eta^5\text{-}C_7H_7)Fe(CO)_2{}^+O^-(Al)$ species appear immediately after impregnation with the Fe–Co complex and its concentration increases during the 12 h drying period. No $(\eta^5\text{-}C_7H_9)Fe(CO)_2{}^+$ appears immediately after impregnation with $(\eta^4\text{-}C_7H_8)Fe(CO)_3$, however the surface anchored cationic species forms during the 12 h drying period in vacuum. This behaviour

appears to reflect the greater reactivity of the Fe–Co complex.

Physisorbed $(\eta^3\text{-}C_7H_7)Co(CO)_3$

As indicated before, $(\mu\text{-}C_7H_7)FeCo(CO)_5$ decomposes on an alumina surface without the formation of any surface species containing a cobalt carbonyl fragment. Even when $(\eta^3\text{-}C_7H_7)Co(CO)_3$ is contacted with alumina and physisorbed $(\eta^3\text{-}C_7H_7)Co(CO)_3$ can be detected on the surface immediately after impregnation (Fig. 3), during the standard 12 h drying period the cobalt centre is completely decarbonylated.

A special case: surface reactions of $(\mu\text{-}C_7H_7)FeCo(\mu\text{-}CO)(CO)_4$ at very low surface coverage

In experiments studying surface chemistry on oxide supports or when modelling precursor–support interactions of catalytic interest, the metal loading on the surface usually is between 0.5–2 monolayer coverage. In our case, the normal metal loading was about 0.5%, which translates to a coverage of about one monolayer. However with $(\mu\text{-}C_7H_7)FeCo(\mu\text{-}CO)(CO)_4$, experiments with extremely low, 0.05% metal loading, corresponding to a coverage of 0.1 monolayer, were also performed. At such a low coverage the molecules on the surface can occupy the most active sites, and there is a higher probability for interaction with more than one adjacent surface site, at the same time. Therefore, surface reactions may follow a somehow different pathway than on highly covered surfaces.

Indeed, at the onset of the reaction of $(\mu\text{-}C_7H_7)\text{-}FeCo(\mu\text{-}CO)(CO)_4$ with alumina a highly distorted $(\mu\text{-}C_7H_7)FeCo(\mu\text{-}CO)(CO)_4$ molecule appears (see Fig. 8(b)) which was not observed in experiments with high metal loading. The presence of a non-symmetrical bridging CO ligand between Fe and Co indicates that the Fe–Co skeleton is preserved in this molecule. The bridging CO appears to be closer to the iron atom than to cobalt. In the next step the distorted molecule splits and forms $(\eta^4\text{-}C_7H_8)Fe(CO)_3$ (via protonation of the nascent $C_7H_7Fe(CO)_3^-$ anion) and the Co must already interact strongly with the surface via Co–O–Al bonding. It is also possible that the bimetallic entity can be temporarily stabilized by formation of weak hydrogen bonding between terminal carbonyls and adjacent surface hydroxyls. Such interactions could possibly promote the formation of the other observed surface species, $(\eta^5\text{-}C_7H_7)Fe(CO)_2^+$.

Further differences in surface reactions can be discovered when the spectra of Figs. 2 and 3 (high metal loading) are compared with the corresponding experiments with low metal loading, Figs. 4 and 5. While in the case of high metal loading only two sets of bands were found, the first set being assigned to physisorbed $(\eta^4\text{-}C_7H_8)Fe(CO)_3$ and the second to chemisorbed $(\eta^5\text{-}C_7H_7)Fe(CO)_2^+O^-$ (Al) species, at low metal loading further sets of bands could be located in the difference spectra of Fig. 4(a). This implies the occurrence of more than two surface carbonyl species in the latter case. These additional species are, however, at very low concentration and they probably represent differently bonded versions of the two main species.

As a final comment it must be noted that even the frequencies of the two main surface species, $(\eta^4\text{-}C_7H_8)Fe(CO)_3$ and $(\eta^5\text{-}C_7H_7)Fe(CO)_2^+O^-$ (Al), and their thermal behaviour are not perfectly matched between the two sets of experiments with different metal loading. The following points can be made.

(i) With low metal loading, the concentrations of the two main surface species, physisorbed $(\eta^4\text{-}C_7H_8)\text{-}Fe(CO)_3$ and surface anchored $(\eta^5\text{-}C_7H_7)Fe(CO)_2^+\text{-}O^-$ (Al) at low temperatures are similar. However, in the case of high metal loading, the concentration of the dicarbonyl species is much lower than that of $(\eta^4\text{-}C_7H_8)Fe(CO)_3$.

(ii) The position of the bands assigned to physisorbed $(\eta^4\text{-}C_7H_8)Fe(CO)_3$ appear at lower frequencies in the case of low metal loading. The apparent 'e' band is most affected, being red shifted by some $16\text{--}22\ cm^{-1}$. The same holds true for the bands assigned to the surface anchored $(\eta^5\text{-}C_7H_7)Fe(CO)_2^+O^-$ (Al). This probably means that the carbonyl groups of these species at low metal loading form stronger bonds with surface active hydroxyl sites than in the case of high metal loading.

(iii) The thermal stability of the surface species with low metal loading is in general higher than with high metal loading, the carbonyl species being detected up to 573 K under vacuum and 533 K in a dihydrogen atmosphere. Furthermore the thermal stabilities of the two main species depend considerably on the atmosphere being used during the thermal treatment. Under an H_2 atmosphere, there is dramatic difference in their behavior. The bands due to $(\eta^5\text{-}C_7H_7)Fe(CO)_2^+\text{-}O^-$ (Al) start to decrease in intensity already at 323 K, and above 448 K they are not detectable, while $(\eta^4\text{-}C_7H_8)Fe(CO)_3$ exists up to 533 K. This behavior supports our assignment of $(\eta^5\text{-}C_7H_7)Fe(CO)_2^+O^-$ (Al) as being in an oxidized form and therefore less stable under reducing conditions. On the other hand, the lack of positive peaks in the difference spectra of Fig. 5(b) (around 2047 and 1960–70 cm^{-1}) indicates that $(\eta^5\text{-}C_7H_7)Fe(CO)_2^+O^-$ (Al) does not convert via reduction into the species assigned to the 2047 and 1960–70 cm^{-1} bands. Such a conversion would be expected if the latter species was a dicarbonyl of non-oxidized iron, just like in the case of ruthenium where interconversion of the dicarbonyls, $Ru^{2+}(CO)_2\text{--}Ru^0(CO)_2$, occurs upon reduction–oxidation cycles [5]. The lack of conversion supports our suggestion that, with low metal loading,

the species that is stable in an H_2 atmosphere is the same tricarbonyl compound, $(\eta^4\text{-}C_7H_8)Fe(CO)_3$, as the one in the experiments with high metal loading. Conversely, the high stability of the $(\eta^5\text{-}C_7H_7)Fe(CO)_2^+\text{-}O^-(Al)$ in vacuum, which represents an oxidative rather a reductive environment, supports our contention that the species is indeed one where the iron atom is in an oxidized state.

The lowering of the frequencies of both main species in the case of low metal loading may be due to the possibility that at low coverage the surface adsorbed species can form a larger number of hydrogen bonds more easily with the acidic hydroxo groups than at high coverage. The lowering of the frequencies may also be due to an electronic effect. At very low coverage the electron density on the metal must be higher than at complete coverage and this causes enhanced backdonation and hence lowering of the CO stretching frequencies. This last effect can also be responsible for the higher stability of the carbonyls at low surface coverage.

The significant dependence of the CO stretching frequencies on the surface coverage calls our attention to a phenomenon which is well known in the case of CO adsorption on metal surfaces, where vibrational and electronic interactions of the adsorbed CO molecules cause significant changes in CO stretching frequencies. Similar observations appear to be much less well documented for more complex surface species other than linearly adsorbed mono-carbonyls.

Acknowledgements

References

1 S. Dobos, Nunziante-Cesaro and B. V. Lokshin, *J. Mol. Struct.*, *174* (1988) 325.
2 S. Dobos and A. Beck, *Inorg. Chim. Acta*, *178* (1990) 163.
3 S. Dobos, B. V. Lokshin and S. G. Kazarian, *Inorg. Chim. Acta*, *179* (1991) 255.
4 S. Dobos, I. Böszörményi, J. Mink and L. Guczi, *Inorg. Chim. Acta*, *120* (1986) 135.
5 S. Dobos, I. Böszörményi, J. Mink and L. Guczi, *Inorg. Chim. Acta.*, *120* (1986) 145.
6 R. Nakamura, A. Oomura, N. Okada and E. Echigoya, *Chem. Lett.*, (1982) 1463.
7 R. L. Schneider, R. F. Howe and K. L. Watters, *Inorg. Chem.*, *23* (1984) 4593.
8 R. L. Schneider, R. F. Howe and K. L. Watters, *Inorg. Chem.*, *23* (1984) 4600.
9 R. Alves, D. Ballivet-Tkatchenko, G. Coudurier, N. Duc Chau and M. Santra, *Bull. Soc. Chim. Fr.*, (1985) 386.
10 M. C. Connaway and B. E. Hanson, *Inorg. Chem.*, 25 (1986) 1445.
11 N. Homs, A. Choplin, P. R. de la Piscina, L. Huang, E. Garbowski, R. Sanchez-Delgado, A. Theolier and J.-M. Basset, *Inorg. Chem.*, 27 (1988) 4030.
12 F. Edelmann, D. Hager and J. Takats, manuscript in preparation.
13 L. Kruczynski and J. Takats, *Inorg. Chem.*, *15* (1976) 3140.
14 R. B. King and M. B. Bisnette, *Inorg. Chem.*, *3* (1964) 785.
15 J. E. Mahler, D. A. K. Jones and R. Pettit, *J. Am. Chem. Soc.*, *86* (1964) 3589.
16 (a) R. Burton, L. Pratt and G. Wilkinson, *J. Chem. Soc.*, (1961) 594; (b) H. J. Dauben and D. J. Bertelli, *J. Am. Chem. Soc.*, *83* (1961) 497.